

Contrast enhanced MR angiography of the thoracic aorta: comparison of ECG-gated techniques at 3T

R. P. Lim¹, R. Avery¹, M. Bruno¹, D. Mossa¹, G. McNeal², Y. Natsuaki², and M. B. Srichai¹

¹Radiology, NYU Langone Medical Center, New York, NY, United States, ²Siemens Healthcare, United States

Introduction:

3D T1-weighted contrast-enhanced MRA (CE-MRA) is routinely used for non-invasive evaluation of the thoracic aorta. However, competing demands of high spatial resolution and fast (breath-hold) acquisition often preclude ECG-gating, leading to motion artifact at the aortic root¹. ECG-gated CE-MRA is feasible, but acquires 1 partition per heart beat with standard Cartesian acquisition, prolonging scan time due to wasted "dead" time prior to the next cardiac cycle, often exceeding breath-hold capabilities². We evaluate an ECG-gated CE-MRA sequence that utilizes alternative Cartesian k-space sampling whereby adjacent k_x and k_z points are acquired in a zigzag pattern per heart beat (Fig 1) to improve scanning efficiency and co-ordinate contrast timing with optimal cardiac phase acquisition, and compare it to our standard clinical gated CE-MRA technique.

Methods:

8 patients (6 male, mean 42y, mean heart rate 61bpm) underwent CE-MRA at 3T (Verio, Siemens Healthcare). After informed consent, patients underwent a two-injection protocol with standard ECG-triggered CE-MRA (S-MRA) and zigzag (Z-MRA) ECG-gated CE-MRA (IPR #573: Gated CE MRA, Siemens Healthcare, Germany) performed in random order. 0.075 mmol/kg Gd-DTPA was used for each injection (total 0.15mmol/kg per patient). Sagittal oblique acquisitions were performed. Arterial contrast timing was based on a timing run and standard formula³. Patients were instructed to breath-hold, followed by shallow breathing if they could no longer suspend respiration for the scan duration. S-MRA parameters were: TR/TE 1 R-R/2.1ms, FA 17°, FOV 400mm, 1.6x1.6x2.4mm true resolution, linear encoding, trigger delay 175ms. Z-MRA parameters had matched spatial resolution and FOV with other parameters: TR/TE 1 R-R/1ms, FA 20°, time to center (TTC) approximately 4.5s, TTC per heartbeat ($k_y=0$) acquired at 353ms post-trigger, 3-5 k_z loops per heartbeat (heart-rate dependent). 6/8 partition and phase partial Fourier, and a parallel imaging factor of 2 were used for both sequences. Images were independently reviewed by a blinded cardiologist and radiologist. Image quality (IQ) (0=non-diagnostic, 1=satisfactory, 2=good, 3=excellent), artifacts (0=non-diagnostic, 1=severely limiting, 2=mildly limiting, 3=not limiting, 4=no artifact) and pathology were recorded for 8 arterial segments (sinuses of Valsalva, sinotubular junction (STJ), ascending/arch/descending/diaphragmatic aorta, coronary artery origins, great vessels). Orthogonal diameters were measured at each segment.

Results:

256 segments (128 x 2 readers) were evaluated. Ascending aortic aneurysms (n=2) and a coarctation (n=1) were diagnosed with both techniques. No scans were considered non-diagnostic (Fig 2). Average scan time was significantly higher for S-MRA compared to Z-MRA (44.8±9.5s versus 15.7±3.8s, respectively, $p < 0.001$). Image quality was slightly higher for S-MRA compared to Z-MRA (3.2 versus 3.0, respectively, $p = 0.04$). Highest IQ scores were recorded for segments beyond the ascending aorta for both sequences. STJ/ coronary origin IQ scores and STJ artifact scores were significantly superior for S-MRA, with no other significant differences between sequences.

For artifact, mean scores were slightly higher for S-MRA (3.1±1.2) than Z-MRA (2.9±1.1), but did not achieve statistical significance ($p=0.08$). Segmental IQ scores are summarized in Table 1. Motion was responsible for all artifact scores of 0 or 1 (non-diagnostic and severely limiting). Motion artifact rendered 11/256 (4.3%) segments unevaluable (S-MRA, n=8; Z-MRA, n=3), with 8/11 at coronary artery origins. 23/256 (9%) segments scored 1 for artifact (S-MRA, n=10; Z-MRA, n=13), 11/23 were coronary artery origins (Z-MRA, n=9), and 5/23 sinus of valsalva segments (Z-MRA, n=4). Orthogonal diameter measurements were averaged and compared without meaningful difference in any segment (table 2). Bland-Altman analysis revealed a mean measure difference (Z-MRA minus S-MRA) in aortic diameter of 0.011±0.33 cm between the techniques. Kappa coefficients for diameter measurements showed moderate to substantial agreement (0.49-0.75) between readers for all segments, for both sequences.

Conclusion:

Our preliminary results demonstrate that diagnostic quality ECG-gated Z-MRA is feasible in reasonable breath-hold times in a clinical population. Results in terms of image quality, artifacts and aortic diameter measurements are comparable to standard ECG-gated MRA that uses a 1 partition per heartbeat approach, with considerable decrease in scan time. However, motion at the aortic root was responsible for the majority of non-diagnostic and severely motion-affected segments for both sequences. Further optimization of Z-MRA k-space sampling strategies tailored to patient heart rate, coupled with aggressive image acceleration, may engender further gains in aortic root image quality within comfortable breath hold scan times.

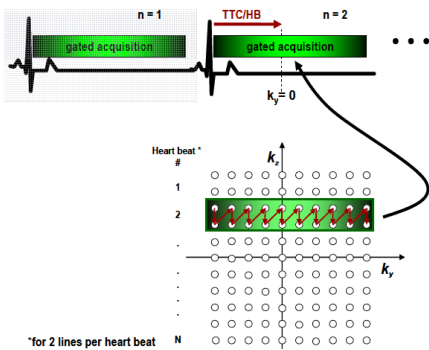


Fig 1 (left): Z-MRA k-space sampling strategy: k_y and k_z datapoints are acquired in a zigzag pattern that improves scanning efficiency (figure from Siemens)

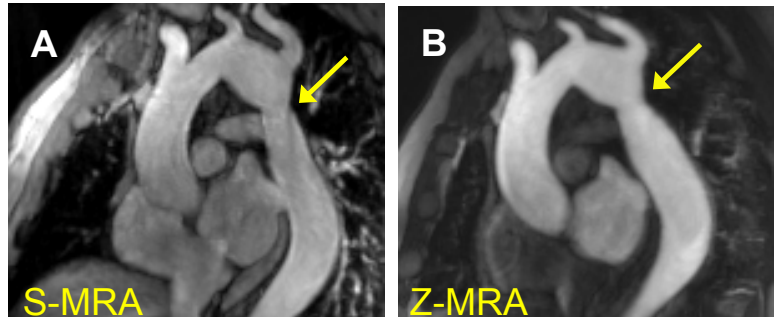
Fig 2 (right):
52 year old male with aortic coarctation (arrows). Thin MIP images A) S-MRA (TA 44s); B) Z-MRA (TA 19s) of good image quality.

Table 1. Image quality scores.

Segment	S-MRA	Z-MRA	P value
Sinuses	3.0±1.1	2.3±0.9	0.07
STJ	3.1±1.0	2.3±0.7	0.03
Ascending aorta	3.3±1.0	2.7±0.7	0.07
Arch	3.6±0.7	3.8±0.4	0.37
Descending aorta	3.6±0.7	3.8±0.4	0.38
Diaphragmatic aorta	3.6±0.8	3.9±0.3	0.16
Coronary origins	2.1±1.0	1.6±0.5	0.03
Great vessels	3.4±1.0	3.8±0.4	0.19
Overall	3.2±1.0	3.0±1.0	0.04

Table 2. Average diameter scores.

Segment	S-MRA	Z-MRA	P value
Sinuses	3.7±0.8	3.7±0.8	0.05
STJ	3.3±0.8	3.2±0.8	0.049
Ascending aorta	3.3±0.7	3.3±0.7	0.07
Arch	2.6±0.5	2.6±0.5	0.74
Descending aorta	2.3±0.4	2.3±0.3	0.13
Diaphragmatic aorta	2.2±0.3	2.1±0.3	0.13
Overall	2.9 ± 0.8	2.9 ± 0.8	0.08



References:

1. Potthast S et al. J Magn Reson Imaging 2010; 31: 177-84.
2. Birely II WR et al. J Magn Reson Imaging 2007; 26:1480-1485.
3. Earls JP et al. Radiology 1996; 201: 705-10